An Improved RF-Sheath Boundary Condition and Implications for ICRF Modeling

J. R. Myra

Lodestar Research Corporation, Boulder, CO, USA

H. Kohno

Kyushu Institute of Technology, Iizuka, Fukuoka, Japan

September 2016

26th IAEA Fusion Energy Conference, Kyoto, Japan, 17 -22 October 2016, paper IAEA-CN-234/TH/P4-31

DOE-ER/54392-83, ER/54823-18 LRC-16-167

LODESTAR RESEARCH CORPORATION

2400 Central Avenue

Boulder, Colorado 80301

An Improved RF-Sheath Boundary Condition and Implications for ICRF Modeling

J.R. Myra [1] and H. Kohno [2]

[1]Lodestar Research Corporation, Boulder, Colorado, USA
[2]Kyushu Institute of Technology, Iizuka, Fukuoka, Japan

E-mail contact of main author: jrmyra@lodestar.com

Abstract. Heating and current drive by ion cyclotron range of frequency (ICRF) waves are expected to play an increasingly important role as tokamak research progresses towards the reactor regime. The basic heating and current drive interactions of ICRF waves with the core plasma are well understood, and sophisticated modeling tools are available. In contrast, the ability to understand, predict and control ICRF interactions with the scrape-off layer plasma is relatively poor. To improve the fidelity of global ICRF codes for this purpose, a newly improved rf sheath boundary condition has been formulated. Extending previous work, which employed a capacitive limit, the new boundary condition generalizes the formulation to a complex sheath impedance which additionally describes the effective sheath resistance at rf frequencies. The latter is important for modeling localized rf power deposition which could potentially cause damaging plasma material interactions. A generalized sheath model has been developed and is described by four dimensionless parameters: the degree of sheath magnetization, the magnetic field angle with the surface, the rf field strength and the degree of ion mobility set by the wave frequency. Characterization of the sheath impedance in the full parameter space is presented with the goal of a self-contained boundary condition package that can be used in global rf codes to describe boundary interactions. The special case where the magnetic field is normal to the surface has been employed in a model for testing and verification. Power dissipation at the surface is calculated in this model.

1. Introduction

Waves in the ion cyclotron range of frequencies (ICRF) have important applications in fusion devices today for heating and current drive. These applications are expected to continue based on ICRF cost effectiveness and good access to reactor regime plasmas. While ICRF waves have been successfully used in many experiments, there are some regimes in which excessive interactions with the antenna and/or boundary plasma are observed. Understanding where these regimes occur in parameter space, and how to predict and avoid them, is an important challenge to the ICRF community. This paper aims to improve the fidelity of global ICRF codes for the purpose of modeling rf interactions with material surfaces in the plasma boundary. We propose and investigate the properties of a generalized rf sheath boundary condition (BC). Our work complements and extends a community-wide effort to understand, model and minimize interactions of ICRF waves with the antenna structure and also with more distant walls and limiters. [1-21]

Boundary interactions are largely governed by rf-sheaths which form on the Debye scale, and direct simulation of this microscale physics in macroscale rf codes is not practical. For this reason an rf-sheath boundary condition has been used in a number of investigations. [2,5,6,9,11-13,15] In particular, the importance of sheath plasma wave resonances, [6, 11,15] tangency points of the

surfaces and magnetic field, [12] and fast-wave to slow-wave conversion depending on surface shaping [13] were pointed out. "Rectified" dc sheath voltages resulting from the sheath interactions were calculated. These sheath voltages, which greatly exceed the electron temperature T_e in realistic applications, can be responsible for ion sputtering, material erosion, impurity release, and localized parasitic loss of rf power to the surface, which can cause material damage.

The sheath BC proposed in [5] was based on the capacitive limit which is strictly applicable only when $\omega >> \omega_{pi}$ where ω is the rf wave frequency and ω_{pi} is the local ion plasma frequency. In this limit, the rf current across the sheath of width Δ is dominated by displacement current; particle currents are negligible. Furthermore, in previous studies, the sheath width Δ was either specified, or if calculated self-consistently, was assumed to be given by the Child-Langmuir law for perpendicular or strongly magnetized sheaths. Recent work, [16] briefly reviewed in Sec. 2, has established a generalization of these conditions and leads to a procedure for calculating the sheath impedance (or equivalently admittance) including both displacement J_d, and particle (electron J_e and ion J_i) currents for general oblique angle rf sheaths immersed in a magnetic field. The generalized sheath BC is discussed in Sec. 3, the sheath admittance is characterized over its parameter space in Sec. 4 and an example of wave-boundary interaction using the generalized sheath BC is presented in Sec. 5. An important consequence of the generalized sheath BC is that the complex sheath impedance includes both capacitive and resistive responses. The latter is important for modeling localized rf power deposition.

2. Sheath admittance: the microscale model

The generalized Debye-scale sheath model for the sheath impedance z, or equivalently the admittance y =1/z, is characterized by four dimensionless input parameters [16]

$$\hat{\Omega} = \Omega / \omega_{pi0}, \quad b_n = \mathbf{B}\cdot\mathbf{n} / B, \quad \hat{\omega} = \omega / \omega_{pi0}, \quad \hat{V} = e\left|V_{pp,rf}\right| / T_e \qquad (1)$$

which describe respectively the degree of sheath magnetization (note that $\hat{\Omega} = \lambda_{d0} / \rho_s$ where $\rho_s = (T_e/m_i)^{1/2}$ is the ion sound radius), the magnetic field angle with the surface, the degree of ion mobility, and the rf field strength. Here all quantities are evaluated at the entrance to the magnetic presheath, [22] **n** is the unit normal to the surface, pointing into the plasma, **B** is the background magnetic field, $|V_{pp,rf}|$ is the amplitude of the peak-to-peak rf voltage at the entrance to the sheath, Ω is the ion cyclotron frequency and ω_{pi} is the ion plasma frequency. The value of $|V_{pp,rf}|$ is to be calculated from a global code (self-consistently) using the sheath BC.

The micro-scale model [16] consists of two parallel plates separated by a distance $L >> \lambda_d$, filled with plasma and permeated by a constant magnetic field oriented at an arbitrary angle. The plates are dc grounded and driven with equal and opposite sinusoidal rf voltages, $V_{rf} \equiv \xi \cos \omega t \equiv \xi \cos \varphi$. Far from the plates, the plasma is allowed to seek a self-consistent potential which determines the dc voltage drop $\Phi_{0,dc}$ from the plasma to the plates. The response of the electrons on the scale of the sheath is described by the Maxwell-Boltzmann relation, valid when $\omega\Delta < v_{te}$ where v_{te} is the electron thermal velocity. From the time-dependent, periodic solutions of this model, the

sheath admittance, y = 1/z, can be calculated by evaluating the ratio of the rf sheath current $J = J_e + J_i + J_d$, to the rf voltage drop across the sheath V_{rf} at frequency ω.

Determination of the upstream plasma potential Φ_0, and consequently the sheath voltage drop, in general depends on the external circuit. For the present dual-plate model, no net current (summed over both plates) can leave the plasma and we find the approximate result

$$\Phi_0 = \ln\left(\mu \cosh(\xi \cos \omega t)\right) \tag{2}$$

where $\mu = [m_i/(2\pi m_e)]^{1/2}$. Throughout this section and Sec. 4 we work in a Debye normalization with density, potential, length and time normalized respectively to the upstream density n_{i0}, T_e/e, λ_{d0} and $1/\omega_{pi0}$; we drop the super^ notation for normalized variables where no confusion can arise. Eq. (2) assumes the component of upstream ion flow velocity perpendicular to the plate is b_n (i.e. the upstream parallel velocity $u_{\|0}$ is sonic). [22] It also assumes Boltzmann electrons and is exact in the limit $\omega << 1$; however, it is accurate to better than 15% for all ω. As is clear from Eq. (2), the time average $\Phi_{0,dc}$ includes contributions from the rectified rf voltage, and is important for sputtering and erosion: it accelerates ions into the surface. For large V_{rf}, i.e. $\xi >> 1$, Φ_0 and its time average are roughly proportional to V_{rf}; for $\xi << 1$, Φ_0 takes its usual value for a static thermal sheath.

3. Generalized sheath boundary condition for macroscale simulations

The sheath impedance given by the microscale model may be applied in macroscale codes (space scales >> λ_d) using the sheath boundary condition

$$\mathbf{E}_t = \nabla_t (J_n z_s) \tag{3}$$

Here $\mathbf{E}_t$ is the tangential (to the surface) rf electric field, ∇_t is the tangential projection of the gradient, J_n is the normal (to the surface) rf current density and z_s is the complex sheath impedance expressed in CGS units, $z_s = \hat{z}\, 4\pi\lambda_{d0}/\omega_{pi0}$. Both $\mathbf{E}_t$ and J_n are to be evaluated at the sheath entrance; effectively the boundary on the global scale.

Since z_s depends on $|V_{rf}|$ at the sheath entrance and this depends on the global field pattern, which in turn depends on Eq. (3), the micro- and macro-scale problems are coupled. The coupling is in general nonlinear in $|V_{rf}|$, even when harmonic generation in the sheath is neglected in the macroscale simulation. In the capacitive sheath limit, this nonlinearity has been shown to give rise to field enhancements at the sheath-plasma resonance. [6, 11,15]

The significance of modeling the generalized, complex sheath impedance is not only to improve the fidelity of sheath simulations over a wider range of the parameters in Eq. (1), but also to enable the calculation of localized rf power deposition in global codes

$$\frac{P}{A} = \frac{1}{2}\left|J_n\right|^2 \mathrm{Re}(z_s) \tag{4}$$

where P/A is the time-averaged rf sheath power deposited per unit area.

4. Characterization of the sheath admittance

For a practical and convenient implementation of the sheath BC in global codes it is advantageous to have a tabulation or multidimensional fit of the sheath admittance $y(\Omega,\omega,b_n,V)$. Although a brute force tabulation in this four-dimensional Debye-normalized space is possible, we will see that analytical analysis and understanding is highly beneficial. Asymptotic results are available in many limiting cases. These limits are not only important for understanding but they can also be employed to construct functional fits across regimes.

The contributions to the (Debye normalized) rf admittance at frequency ω from electron, displacement and ion currents are given by projecting out the corresponding Fourier contributions

$$y = \frac{\langle JV_{rf} \rangle}{\langle V_{rf}^2 \rangle} - \frac{i\omega \langle J\dot{V}_{rf} \rangle}{\langle \dot{V}_{rf}^2 \rangle} \tag{5}$$

where $\dot{V}_{rf} = dV_{rf}/dt$ and the quantities inside the <…> are to be time-averaged over an rf cycle using the nonlinear micro-scale model.

The electron current is controlled by the instantaneous potential drop across the sheath. For Maxwell-Boltzmann electrons, the normal component of electron current at the plate is

$$J_e = \mu b_n \exp(V_{rf} - \Phi_0) \tag{6}$$

in Debye units, again assuming $u_{\|0}$ is sonic, i.e. 1 in normalized units. This gives the electron admittance as

$$y_e = \frac{2\mu b_n \langle \cos\varphi \, e^{\xi\cos\varphi - \Phi_0} \rangle}{\xi} \tag{7}$$

where $\varphi = \omega t$ and ξ is the rf amplitude. For the double-sided sheath model, using the approximation of Eq. (2)

$$y_e = \frac{4b_n}{\xi} \left\langle \frac{\cos\varphi}{1 + e^{-2\xi\cos\varphi}} \right\rangle \tag{8}$$

It can be shown that that the asymptotic limits are $y_e = b_n$ for $\xi << 1$ and $y_e = 4b_n/(\pi\xi)$ for $\xi >> 1$.

The displacement admittance is formally the same as in the capacitive sheath model,

$$y_d = -\frac{i\omega}{\Delta} \tag{9}$$

except now the time-averaged sheath width Δ must be computed for an oblique magnetized sheath. The time-averaged non-neutral sheath width is primarily set by the dc potential drop across the sheath, approximately given by Φ_0 for $\xi >> 1$ (The potential drop across the presheath is of order unity.) Thus the scaling of Δ should be given by that of a similarly biased static sheath.

The static biased oblique-angle magnetized sheath has been fully characterized by patching together asymptotic results [23] from various regimes. Detailed fits accurate to a few percent have been obtained and will be presented elsewhere. Qualitatively, simple Padé rationals that give the correct asymptotic power law dependencies are as follows:

$$\Delta = \left(\frac{\Phi}{n_i} \right)^{1/2} \tag{10}$$

$$n_i = \frac{1}{\Phi^{1/2}} \frac{b_n + \Omega_\Phi^2}{1 + \Omega_\Phi^2} \tag{11}$$

where $\Phi \sim \Phi_0$ is the dc potential drop across the non-neutral sheath and $\Omega_\Phi = \Omega \Phi^{1/4}$. Here n_i is the normalized ion density inside the non-neutral sheath, at the wall. Note that the usual Child-Langmuir law is obtained for perpendicular sheaths ($b_n = 1$) and that Φ is order unity or larger because of the thermal sheath which has $\Phi \sim 3$.

The ion admittance is the most complicated to characterize. Detailed fits of numerical results (accurate to a few percent) have been obtained for the perpendicular case and are presented in Fig. 1. New physics enters for the ions when $\hat{\omega}$ is order unity as can occur in high density regions of the SOL. In this case the ions traverse the Debye sheath in a time of order $1/\omega_{pi}$ which is comparable to the wave period; thus they experience a dissipative ion plasma resonance interaction.

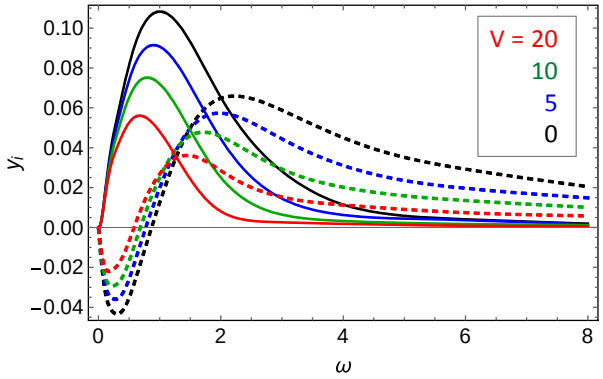

FIG. 1. Variation of the ion contribution to the sheath admittance as a function of frequency and rf voltage across the sheath: Re(y) (solid) and Im(y) (dashed). A dimensionless normalization to λ_{d0}, ω_{pi0} and e/T_e has been employed.

The amplitude and frequency of the resonant-type response can be understood in terms of the average ion density in the sheath (which drops with increasing rf voltage and therefore shifts the ω_{pi} resonance and reduces the rf ion current).

For the general oblique magnetized case, the dynamical ion equations can be solved in the limits of very low frequency where the ions respond to instantaneous potential as if it were dc, and very high frequency where the rf ion response is weak and linear (because of large ion inertia). The resonant case $\omega = \omega_{pi}$ can also be solved approximately. A Padé rational approximation for $\omega > 2\Omega$ that gives approximate asymptotic results is:

$$y_i \sim \frac{n_i}{\Phi^{1/2}} \frac{i\breve{\omega}}{(\breve{\omega}^2 - 1 + i\breve{\gamma}\breve{\omega})} \tag{12}$$

where $\breve{\omega} = \omega / n_i^{1/2}$ (i.e. $n_i^{1/2}$ is ω_{pi} inside the sheath) and $\breve{\gamma} \approx b_n/(n_i\Phi^{1/2})$. Here n_i and Φ are the same as discussed for y_d. See Eqs. (2) (time-averaged) and (11). Eq. (12) is somewhat qualitative: more detailed results and numerical fits will be presented elsewhere.

Fortunately, for many cases of interest for ICRF, y_i makes a relatively small contribution to the total admittance, which is finally given by

$$y = y_e + y_i + y_d \tag{13}$$

5. Wave propagation with the generalized sheath BC

We have begun to investigate wave propagation physics with the generalized sheath BC, at present for the perpendicular sheath case. Previously we showed that the theory conserves energy between rf sheath dissipation and the waves.[16] In the (high density) regime of evanescent slow waves, the complex sheath impedance provides dissipation for the sheath-plasma wave resonance. In this case it can be shown that power is transferred between the sheath-plasma waves and the rf waves in the volume through a cross term in the Poynting flux which describes evanescent tunneling. Details will be presented elsewhere.

In the (low SOL density) case of propagating slow waves, some of the slow waves are reflected at the wall by the sheath and some are absorbed. For a semi-infinite-domain 1D slow-wave (SW) model where the SW propagates in the x-direction along B and impacts a sheath at perpendicular incidence, it can be shown that the fraction of power absorbed by the sheath is given by

$$P_{sh} = 1 - |A|^2 \tag{14}$$

where the reflection coefficient is

$$A = \frac{\rho - 1}{\rho + 1}, \quad \rho = \frac{\omega z_s k_x^2 \varepsilon_\perp}{4\pi k_z} \tag{15}$$

For $|\rho| << 1$ we have $A = -1$ which corresponds to a conducting BC, while for $|\rho| >> 1$ we have $A = 1$ which is an insulating BC. In both of these cases $|A| = 1$, and the result is a standing wave: there is no Poynting flux or power dissipation in the sheath. For complex z_s the Poynting flux and power dissipation are finite, maximizing at $\rho = 1$. However, total power absorption, $\rho = 1$, is not possible in this case because it requires $\varepsilon_\perp > 0$ for SW propagation, i.e. $\omega^2 > \omega_{pi}^2 + \Omega^2$ but also $\omega < \omega_{pi}$ for a dominantly real sheath impedance, Im y_d < Re(y_i) + y_e. Nevertheless partial sheath power absorption typically occurs.

This is illustrated in Fig. 2 for a perpendicular sheath case using a 1D model with a sheet current antenna at x = 0.8 m and sheath BCs at x = 0 and 1.0 m; note that the plots shown here are obtained from the physical quantities at the x = 1.0 m sheath. Other parameters are $\mathbf{B}_0 = B_{0x}$ =

1T, $k_y = 0$, $k_z = 10.8\ m^{-1}$, $\omega/2\pi = 80$ MHz, $T_e = 15$ eV and two values of the constant density: $n_e = 3.0 \times 10^{17}$ and $1.5 \times 10^{18}\ m^{-3}$.

Fig. 2(a) shows that, depending on plasma conditions (in particular n_e in this example), the capacitive and generalized sheath BCs can result in either similar or very different rf sheath voltages. The higher density case has smaller ω/ω_{pi} and as a result is more disparate from the capacitive limit which applies when $\omega/\omega_{pi} >> 1$. The rf power absorption per unit area at the surface calculated from Eq. (4) is illustrated in Fig. 2(b) for the low and high density cases (generalized sheath BC only). P/A increases with plasma density and of course both it and the sheath voltage increase with antenna current. We have verified that the time-averaged Poynting vector component of the rf waves from the plasma into the sheath is equal to P/A given by Eq. (4).

The normalized sheath impedance (generalized sheath BC) is shown in Fig. 2(c). P/A continues to rise steeply as K_{max} is further increased, approaching 0.8 MW/m^2 for the high n_e case at K_{max} = 700 A/m where the sheath voltage $|V_{rf}| = 120$ V. Further analysis reveals that the large P/A observed in this case is dominated by the electron contribution y_e to Re(z). The dimensionless frequency parameter is $\hat{\omega} = 0.44$ for this case, and the local value, $\breve{\omega}$ in the sheath, is further reduced at high voltage according to Eq. (11). The small value of $\breve{\omega}$ makes the ion contribution small, Eq. (12), while y_e remains independent of ω, Eq. (8). Furthermore, for perpendicular sheaths, the condition for $|y_e| > |y_d|$ at high voltages ($\xi >> 1$) is approximately $\hat{\omega}\hat{\Phi}^{1/4} < 1$. This condition is satisfied here, and results in Re(z) > Im(z).

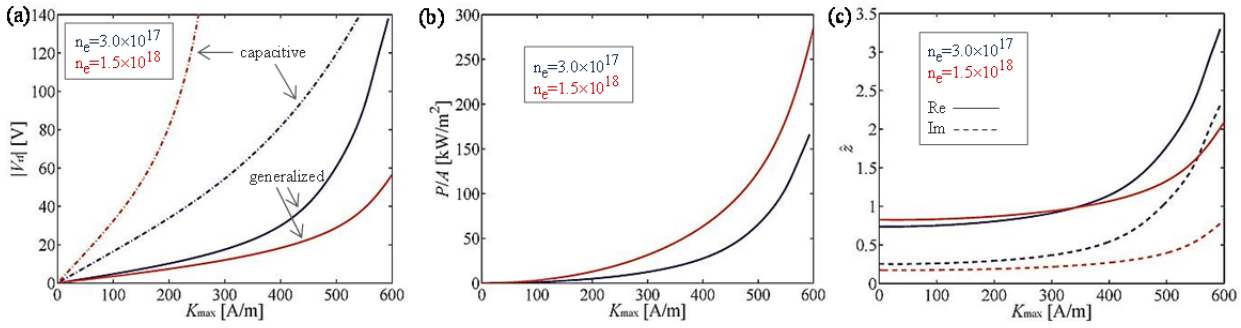

FIG. 2. Dependence of (a) rf sheath voltage, (b) sheath power absorption and (c) dimensionless sheath impedance vs. antenna current for a 1D wave problem using the capacitive (a) and generalized (a) – (c) sheath BC. Densities are $n_e = 3.0 \times 10^{17}$ (dark blue) and $1.5 \times 10^{18}\ m^{-3}$ (red).

6. Summary and conclusions

It is critical to understand, model and thereby avoid the parameter regimes where deleterious interactions between ICRF waves and material boundaries occur. To this end, using a Debye-scale model, we have developed a generalized sheath boundary condition in terms of an effective sheath impedance. This BC can then be used by macroscopic (global) rf codes to predict ion impact energies for sputtering, localized rf power deposition and global parasitic power losses to sheaths.

This paper has first outlined an approach for calculating the dc (rf rectified) sheath voltage, and the electron, ion and displacement contributions to the sheath admittance. All of these rf sheath quantities have then been characterized over the four-dimensional parameter space defined by Eq. (1). We have verified the sheath BC method by applying it to sample 1D macroscopic problems, showing that it leads to self-consistent solutions from which the sheath voltage and power deposition can be calculated. The method generalizes and significantly extends the capacitive sheath BC that has been commonly used up to this point.

Acknowledgement

This material is based upon work supported by the U.S. Department of Energy Office of Science, Office of Fusion Energy Sciences under Award Numbers DE-FG02-97ER54392 and DE-FC02-05ER54823. Discussions with the RF SciDAC team (Center for Simulation of Wave-Plasma Interactions) are gratefully acknowledged.

References

[1] BOBKOV, V., et al., Nucl. Fusion **56** (2016) 084001.

[2] COLAS, L., et al., 25th Fusion Energy Conf., Saint Petersburg (2014) IAEA-CN-221/TH/P6-9.

[3] CORRE, Y., et al., Nucl. Fusion **52** (2012) 103010.

[4] CROMBÉ, K., et al., AIP Conference Proceedings **1689** (2015) 030006.

[5] D'IPPOLITO, D.A., et al., Phys. Plasmas **13** (2006) 102508.

[6] D'IPPOLITO, D.A., et al. Plasma Phys. Control. Fusion **55** (2013) 085001.

[7] FAUDOT, E., Phys. Plasmas **22** (2015) 083506.

[8] JACQUOT, J., et al., Phys. Plasmas **21** (2014) 061509.

[9] JAEGER, E.F., et al., Phys. Plasmas **2** (1995) 2597.

[10] JENKINS, T.G. and SMITHE, D.N., AIP Conference Proceedings **1689** (2015) 030003.

[11] KOHNO, H., et al., Phys. Plasmas **19** (2012) 012508.

[12] KOHNO, H., et al., Phys. Plasmas **20** (2013) 082514.

[13] KOHNO, H., et al., Phys. Plasmas **22** (2015) 072504; ibid **23** (2016) 089901.

[14] MILANESIO, D., and MAGGIORA, R., Phys. Plasmas **21** (2014) 061507.

[15] MYRA, J.R. and D'IPPOLITO, D.A., Plasma Phys. Control. Fusion **52** (2010) 015003.

[16] MYRA, J.R. and D'IPPOLITO, D.A., Phys. Plasmas **22** (2015) 062507.

[17] OCHOUKOV, R., et al., Plasma Phys. Control. Fusion **56** (2014) 015004.

[18] PERKINS, R.J., et al., Phys. Plasmas **22** (2015) 042506.

[19] QIN, C.M., et al., Plasma Phys. Control. Fusion **55** (2013) 015004.

[20] VAN EESTER, D., et al., Plasma Phys. Control. Fusion **55** (2013) 055001.

[21] WUKITCH, S.J., et al., Phys. Plasmas **20** (2013) 056117.

[22] CHODURA, R., Phys. Fluids **25** (1982) 1628.

[23] AHEDO, E., Phys. Plasmas **6** (1999) 4200.